This article has been accepted for publication in IEEE Sensors Journal. This is the author's version which has not been fully edited and content may change prior to final publication. Citation information: DOI 10.1109/JSEN.2024.3419257

Comparative Study of pH Sensors Based on PAni-coated Specialty Optical Fibers

Armando Rodriguez, Guilherme Lopes, Jan Nedoma, *Senior Member IEEE,* Sónia O. Pereira, António J. S. Fernandes, Raphael Jamier, Philippe Roy, Mikel Bravo, Manuel Lopez-Amo, *Senior Member IEEE* and Carlos Marques

***Abstract*— In this paper, we report the analysis of a novel optical fiber pH sensor based in polyaniline coating applied on a trenched core-free (only-bridge) silica fiber. The results are compared to another pH sensor based on side-polished silica fiber. The pH sensitive polymer is synthetized over the fiber sample by means of oxidative polymerization, keeping records of the time where the reaction occurs to improve the sensitivity. The response to pH is enhanced in the case of the trenched core-free bridge fiber due to the higher interaction of the evanescent field with the polyaniline film, thus, the surrounding media. The sensitivity in the linear zone of operation is 1.1 mW/pH, and a total transmittance of 55 % in the pH range of 4.2 to 8.1. The repeatability of both sensors was checked, showing a high capability to perform studies in liquid samples due to its temperature independence, good sensitivity and long-term stability.**

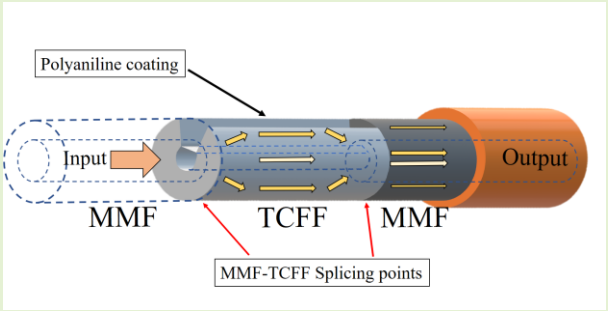

***Index Terms*— Trenched core-free fiber, pH sensor, polyaniline, side-polished fiber.**

I. Introduction

The pursuit of efficient, accurate, and versatile sensing technologies is an important issue in various scientific and industrial domains. Among these, pH sensing stands out as a main parameter influencing diverse fields such as environmental monitoring, biomedical research, and chemical process control [1]. Optical fiber sensors have emerged as promising candidates for pH monitoring due to their inherent advantages including high sensitivity, immunity to electromagnetic and chemical interrelation, and remote operation capabilities.

This work was supported in part by project PID2022-137269OB-C21 funded by MCIN/AEI/10.13039/501100011033 and FEDER "A way to make Europe", and TED2021-130378B-C22 funded by MCIN/AEI/10.13039/501100011033 and European Union "Next generation EU"/PRTR and the Beatriz Galindo BEAGAL18/00116 grant funded by MICINN. (*Corresponding author: Armando Rodriguez*)

Armando Rodriguez, Mikel Bravo and Manuel Lopez-Amo are with Electrical, Electronic and Communication Engineering Dept. and Institute of Smart Cities (ISC), Public University of Navarra, 31006 Pamplona, Spain (e-mail: armando.rodriguez@unavarra.es).

Guilherme Lopes is with CICECO, Physics Department, University of Aveiro, 3810-193, Aveiro, Portugal.

Carlos Marques is with CICECO, Physics Department, University of Aveiro, 3810-193, Aveiro, Portugal and Department of Physics, VSB – Technical University of Ostrava, Ostrava, 70800, Czech Republic.

Jan Nedoma is with Department of Telecommunications, VSB – Technical University of Ostrava, Ostrava, 70800, Czech Republic.

Sónia O. Pereira and António J. S. Fernandes are with I3N, Physics Department, University of Aveiro, 3810-193, Aveiro, Portugal.

Raphael Jamier, Philippe Roy are with XLIM UMR CNRS 7252, University of Limoges, F-87000 Limoges, France.

Several techniques have been developed to meet this common demand for ease. In recent years, different types of sensors have been reported, mostly based on carbon nanotubes [2], potentiometric and capacitive changes [3], [4], [5], micro-electrical mechanical systems [6], CMOS [7] and surface plasmon resonance [8], [9], as the representatives examples.

Optical fibers have been employed as a passive transmission line in a number of the previously discussed techniques (only to transfer light to and from the detecting head [10]), but in a large number of other techniques, they play an active role as optical transducers [11], [12], [13].

In the design and deployment of fiber optic pH sensors, the light must interact with sensitive materials in contact with the outer medium placed in the fiber. The polyaniline (PAni) coating has garnered significant attention due to the good properties of the polymer, such as reversible pH-dependent conductivity and ease of synthesis. For instance, sensors based in PAni and fiber Bragg gratings (FBG), tilted FBG and long-period gratings have been reported [14]. Specifically, a fiber optic pH sensor was developed [15] based on tilted FBG where a coating of PAni was deposited on the fiber's surface, achieving a range of measurement of 2 to 12 with a fast response.

Another optical fiber sensing structure used is the D-shape fiber, where a section the fiber's cladding is polished, exposing the core of this region [16]. This design enhances the interaction of light with the medium to be sensed. Several methods refer to fibers geometrically modified, such as fibers without cladding, but their sensitivity is compromised in most

XXXX-XXXX © XXXX IEEE. Personal use is permitted, but republication/redistribution requires IEEE permission.
See http://www.ieee.org/publications_standards/publications/rights/index.html for more information.
This work is licensed under a Creative Commons Attribution-NonCommercial-NoDerivatives 4.0 License. For more information, see https://creativecommons.org/licenses/by-nc-nd/4.0/

This article has been accepted for publication in IEEE Sensors Journal. This is the author's version which has not been fully edited and
content may change prior to final publication. Citation information: DOI 10.1109/JSEN.2024.3419257

of the cases. D-shape fibers have attracted the attention of researchers as a mechanically stronger structure for sensing [17].

In this paper, we present a comprehensive comparative analysis of two different fiber optic pH sensors, each one employing a distinct configuration and structure. Specifically, we will remark a sensor based on an only-bridge trenched core-free fiber (TCFF) combined with a PAni coating. We will compare its performance with a similar coating of an optical fiber sensor based on a D-shaped optical fiber.

II. Materials and Methods

The study was performed using two different types of sensing optical fibers which provide a platform for efficient light coupling and interaction with the surrounding medium. The first sensor system is based in a side-polished optical fiber from *Phoenix Photonics*®, also called as D-shape as the structure formed in the fiber cladding. The aim is to remove a section of the cladding to gain access to the evanescent field. The polished region length is ~17 mm, following a fiber profile as the one depicted in Fig. 1.

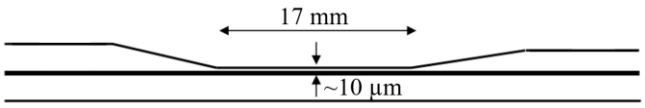

Fig. 1. Profile of D-shape fiber.

The other one is a trenched core-free fiber (TCFF) manufactured by Xlim Institute (France), which has a particular inner structure. It consists of a coreless fiber where a longitudinal portion of cladding is removed, leaving a thin interface between the center of fiber and the external medium that resembles a small suspended bridge. Fig. 2 depicts the microscope picture of the fiber and its dimensions.

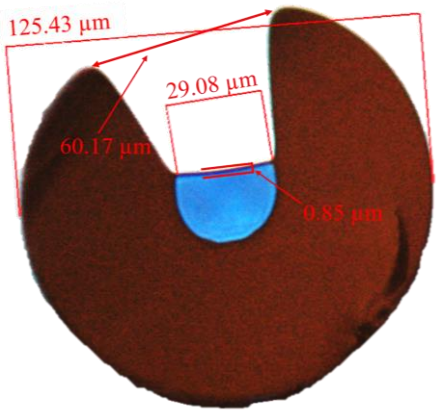

Fig. 2. Microscope photography of THCF.

The open space in the cladding makes it suitable for depositing smart materials or to introduce elements to be measured, interacting with the light traveling either through the hollow core or the cladding.

In both experiments, corresponding to the two different fibers, the same transmissive setup was used, as shown in Fig. 3. There, a Teflon container acts as a fiber holder allowing the PAni section deposited on the fiber to be immersed in the solution to be measured. A halogen light source model LSW7, brand *Sarspec*, has been used, whose maximum power is 7W with an emission range between 380 nm to 2500 nm. The detector is a FLAME-T-UV-vis spectrometer manufactured by *Ocean Optics*, with a detection range of 180 nm to 890 nm and the error margin according to the power resolution is 0.01 Counts. The data was captured via the OceanView spectral analysis software and the traces were processed on a customized software developed in MATLAB.

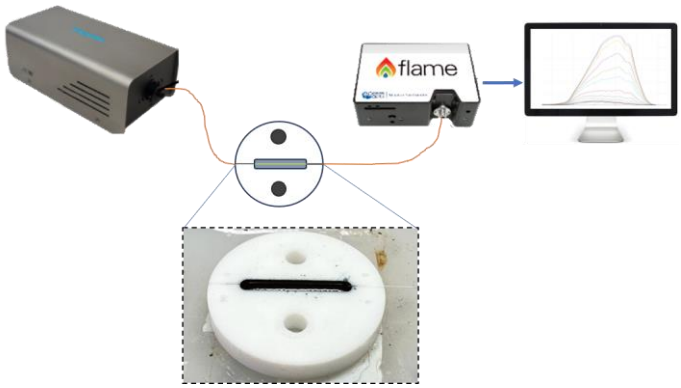

Fig. 3. Experimental setup of the novel fiber-optic pH sensor.

The D-shape fiber was manufactured in a single-mode fiber (SMF) according to technical specification and connected through a FC-APC optical fiber pigtail in both ends. Both the spectrometer and halogen lamp source have SMA connectors in the interfaces with a SMA to FC-PC multimode fiber (MMF) pigtail attached. Thus, an additional APC-PC pigtailed transition was used.

Additionally, the TCFF was spliced to an MMF pigtail in both ends, because of its internal diameter of ~30 µm, being an optimal way to couple the light from the source and to retrieve its transmission spectrum.

A. PAni synthesis

As stated before, PAni was used as the sensitive element to pH variations. This is a polymer that exhibits reversible pH-dependent conductivity, meaning that its electrical conductivity changes in response to variations in pH levels. Three oxidation states of PAni have been identified and all of these structures can exist either in their salt form (protonated) or in their base form (deprotonated), which is accomplished by applying the base form to an acid, as demonstrated in [15], [18], [19].

The PAni layer was synthetized *in-situ* by oxidative polymerization, i.e. in the presence of the D-shape fiber or the TCFF. The procedure was adapted from the work developed by [16]. For this purpose, aniline was used as monomer and ammonium persulfate as oxidizing agent in acidic aqueous solution. Once fixed to the container, that had an estimated capacity of about 400 µL, the surface of the fiber is firstly cleaned with deionized water. Secondly, 300 µL of hydrochloric acid (HCl) at 1.0 M containing aniline (0.133 M) was poured in the container. Subsequently, 100 µL of a solution of ammonium persulfate (0.4 M) prepared with HCl (1.0 M) was added. By thoroughly mixing the solution, the

This work is licensed under a Creative Commons Attribution-NonCommercial-NoDerivatives 4.0 License. For more information, see https://creativecommons.org/licenses/by-nc-nd/4.0/

This article has been accepted for publication in IEEE Sensors Journal. This is the author's version which has not been fully edited and content may change prior to final publication. Citation information: DOI 10.1109/JSEN.2024.3419257

reaction started immediately, rapidly turning from transparent to dark green color.

The polymerization time allows to optimize the thickness of the PAni film on the fiber; thicker may be more sensitive but leads to a slower response or stabilization. Therefore, hysteresis can be observed in the rise and fall of pH levels, as reported elsewhere [16]. In this work, a polymerization time of around 13 minutes was applied in ambient temperature conditions. As example, Fig. 4 depicts the spectral evolution of the only-bridge fiber during the PAni synthesis where the spectral intensity is expressed in terms of optical power (mW).

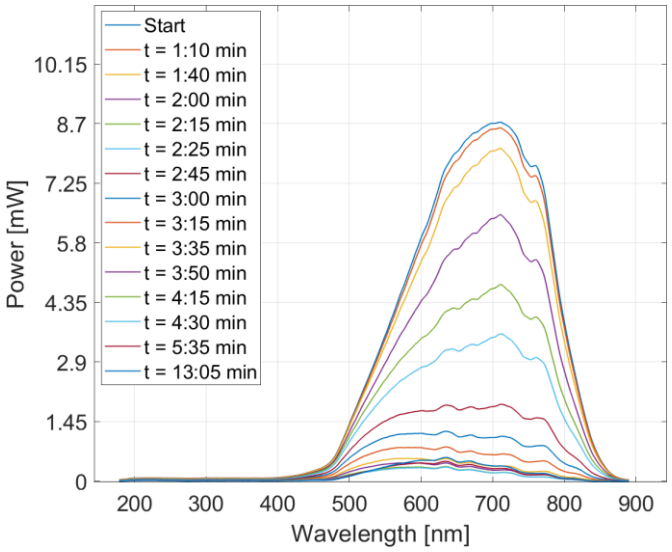

Fig. 4. Spectral evolution of TCFF during polymer synthesis on its surface.

Finally, after the elapsed time, the excess polymer present in the recipient was removed and the coated fiber was washed with deionized water to ensure the complete elimination of reaction precursors.

B. Preparation of pH samples

The experimental tests were carried out using solutions with different pH values. The samples were prepared by varying the ratio between sodium phosphate dibasic heptahydrate ($Na_2HPO_4 \cdot 7H_2O$, *Sigma-Aldrich*) and sodium phosphate monobasic monohydrate ($NaH_2PO_4 \cdot H_2O$, *Sigma-Aldrich*), keeping a constant concentration of 0.01 M. The phosphate ions were dissolved in a solution containing 0.137 M sodium chloride (NaCl) and 0.027 M potassium chloride (KCl). Eight solutions were calculated to maintain the ionic strength in all cases, with pH ranging from 2 to 10. The actual values were measured via pH electrode from *Hanna Instruments*, where the lowest sample recorded pH was 2.75 and the highest was 8.9.

The reference values of each test were measured by placing the coated fibers in a solution of HCl (0.1 M) for more than 5 minutes and capturing the spectrum. Afterwards, the HCl was taken out and the initial sample of calculated pH is added. The procedure is repeated for all pH samples. All tests were performed in a controlled ambient room, with constant temperature of 23 ºC. Moreover, the refractive index (RI) of the solutions were measured an it was confirmed that all the samples present the same RI.

III. 3. Results and Discussion

A. Characterization of fibers without PAni

The fibers were tested before applying the polymer coating in order to check the sensitivity to RI and pH variations. With the aim of characterizing the response of the bare fibers, nine solutions of glucose with different RI were prepared by varying the concentration from 0.1 to 50 %w/v, with RI unit (RIU) values from 1.332 to 1.3861. The RIU values were measured with an Easy R40 instrument from *Mettler Toledo*, which has a measurement range from 1.30 to 1.72 RIU and an accuracy of ±0,0001 RIU. As reference, the RI of air was taken (~1.000).

Fig. 5 represents the transmission spectrum evolution of the D-shape fiber without coating. The transition from air to the glucose solutions is obvious, however, changing the RIU does not affect significative the intensity of the spectrum. The TCFF was also tested and its response was similar.

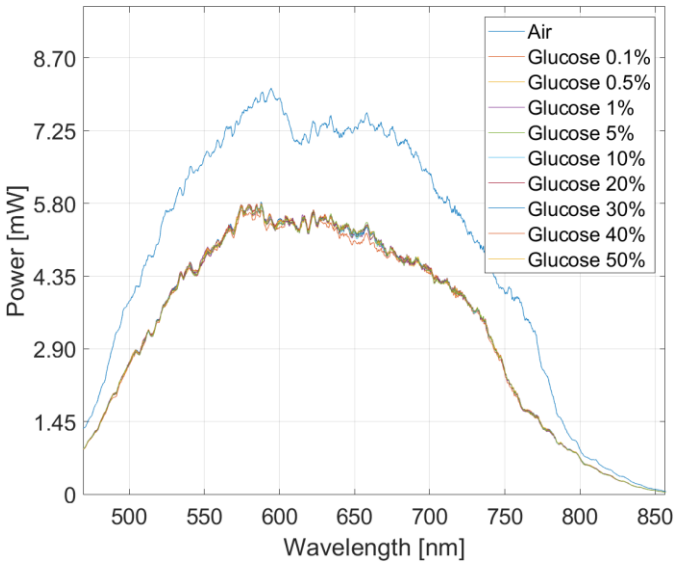

Fig. 5. Spectral response of bare D-shape fiber to RI variation.

Moreover, the sensitivity of bare fibers to pH was also tested. Different pH solutions were used and the spectral response of TCFF is depicted in Fig. 6, where almost no changes in power level are achieved. A similar behavior was observed for the D-shape fiber.

This work is licensed under a Creative Commons Attribution-NonCommercial-NoDerivatives 4.0 License. For more information, see https://creativecommons.org/licenses/by-nc-nd/4.0/

This article has been accepted for publication in IEEE Sensors Journal. This is the author's version which has not been fully edited and content may change prior to final publication. Citation information: DOI 10.1109/JSEN.2024.3419257

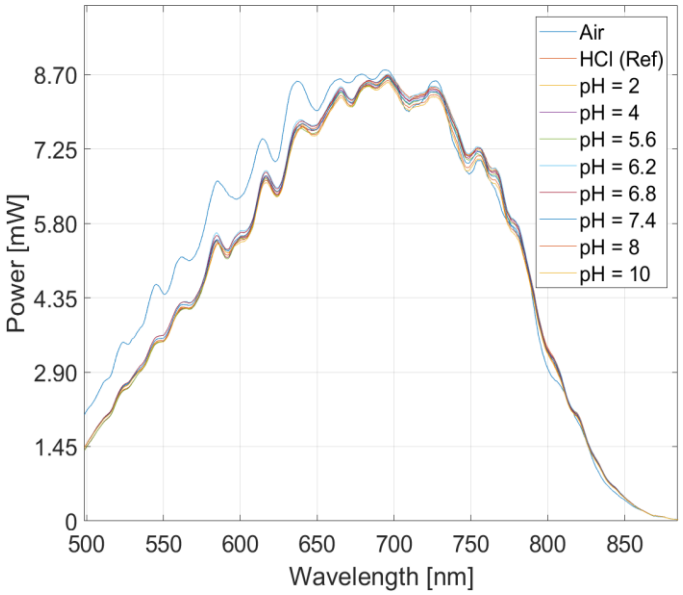

Fig. 6. Spectral response of bare TCFF to pH variation.

In summary, both fibers without the polymer coating demonstrated no substantial reaction to changes in RI and pH. Nevertheless, the sample solutions used in the further experiments were carefully checked to have the same RI value.

B. Measurement of pH with PAni coating

The tests were performed by placing the coated fibers in several pH solutions from the HCl reference sample to pH 9. Each pH solution was placed in the container and after 4~5 minutes of stabilization the data was recorded. As the measurements are based on power variations, it is important to check the stability of the light sources used before each experiment.

Firstly, the TCFF-based sensor was tested and the spectra show a peak around 634.5 nm, decreasing with the increase of pH. This peak was monitored showing only a slight variation up to pH = 4.2 after which the response suddenly increases with an approximate linear trend before getting a slow decreasing rate at the end of the test. The overall response resembles a "S" shape as can be observed in Fig. 7, after performing a Sigmoid fitting to the peak intensity curve, where the ~99.25 % (R^2) of the fit curve represents the actual sensor response. The inset figure depicts the spectral evolution caused by the pH variation.

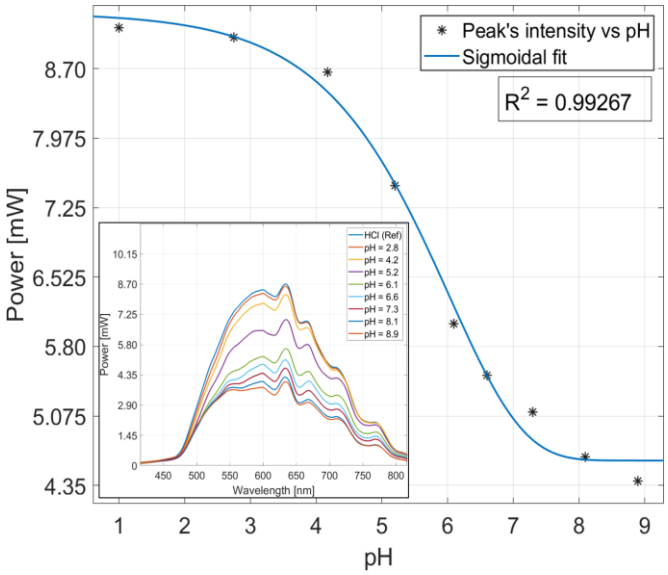

Fig. 7. Response of PAni-coated TCFF sensor to pH variations. *Inset:* spectral evolution.

This mathematical approach typically involves fitting parameters such as the saturation level, slope, and inflection point of the curve [20]. Moreover, it helps to understand valuable insights into the sensor's characteristics, such as its dynamic range, sensitivity, and response kinetics. Thus, the sensitivity value represents how much the response changes with respect to a change in the pH.

Based on this result, the optimal range of operation of this sensor can be defined from pH 4.2 to 8.1, where a linear trend was observed. The obtained sensitivity was about 1.06 mW/pH (R^2 = 0.9604).

Finally, the D-shape fiber-based sensor was also tested. This time, the polymer coating produced a peak around 583.4 nm (see Fig. 8 inset). The response is similar to the previous sensor, showing a ~98.97 % of agreement to the Sigmoidal fit, as depicted in Fig. 8. A linear trend range is also observed but this time between 2.75 and 6.8 (R^2 = 0.9542). A 0.95 mW/pH sensitivity was achieved in this configuration.

This work is licensed under a Creative Commons Attribution-NonCommercial-NoDerivatives 4.0 License. For more information, see https://creativecommons.org/licenses/by-nc-nd/4.0/

This article has been accepted for publication in IEEE Sensors Journal. This is the author's version which has not been fully edited and
content may change prior to final publication. Citation information: DOI 10.1109/JSEN.2024.3419257

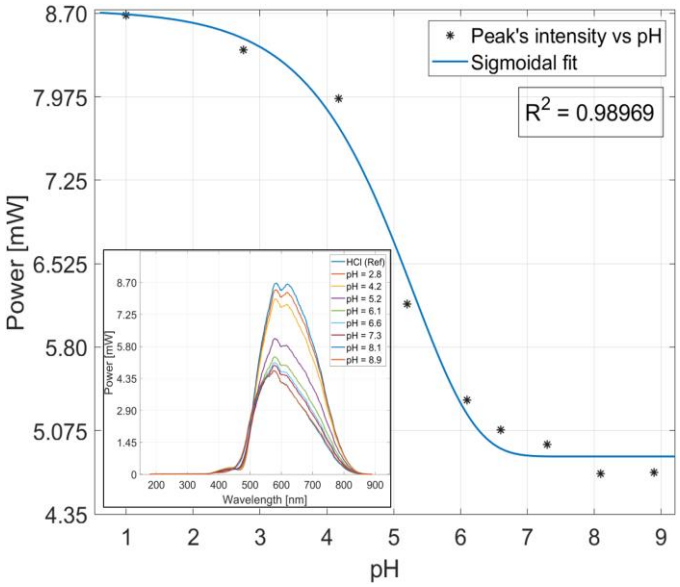

Fig. 8. Response of PAni-coated D-shape sensor to pH variations. *Inset:* spectral evolution.

Although the optimal measurement range is different than the case of TCFF sensor, these results are useful for several applications, including the survival of aquatic life.

C. Repeatability test

The experimental procedures were repeated to assess the suitability of the sensor for multiple uses. Several tests were carried out with a day-gap between every measurement. After finishing each of them, the sensor was rinsed with plenty of deionized water and stabilized using a 0.1 M solution of HCl.

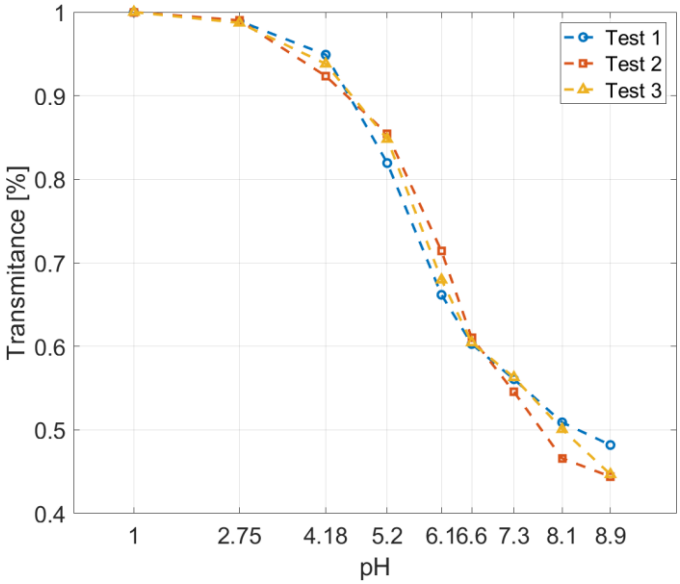

Fig. 9. Repeatability of the TCFF-based sensor.

As demonstrated in [16], the PAni polymer film has showed a high hysteresis when decreasing steps of pH levels. Therefore, the measurement in this work was only performed in increasing steps. Several reports support the findings, stating that this issue is related to different protonation/deprotonation rates in the polymerization of PAni [21].

As a merit figure in the analysis, the normalized transmittance of the sensor was studied for both the initial and the repeatability tests. These shown the same transmittance trend after two days of polymer synthesis.

The peak intensity of spectral response remained at 634.6 nm and despite a decrease in the intensity, the sensor response remained very close. A sensitivity of 1.064 mW/pH (R^2 = 0.9803) and 0.951 mW/pH (R^2 = 0.9674) were determined for the subsequent tests 2 and 3, respectively. Fig. 9 depicts the plot of the experimental results where the optimal operation zone (linear response) was similar in all cases.

The same procedure was repeated with the D-shape fiber-based sensor, as well. The sensor recorded a similar trend up to pH 7.3, in all test. The linear region increases the sensitivity after the first test. However, in the last two experiments the spectral response shifted to a 564.6 nm wavelength peak. And for higher pH values, the transmittance increases (see Fig. 10).

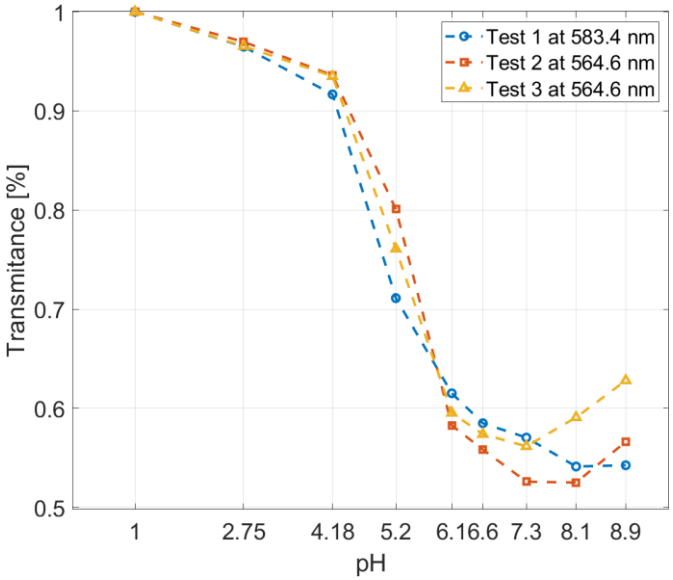

Fig. 10. Normalized transmittance analysis of the repeatability test in D-shape fiber-based sensor.

As can be observed, both sensors achieved a similar trend in the linear operation zone. However, the sensor based on D-shape fiber shows inconsistent behavior at high pH level. In the case of the sensor with TCFF, the response was enhanced in comparison to the first test, which makes it a suitable candidate for multiple usages.

D. Cross-sensitivity test

The previous experimental tests were carried out in a controlled laboratory environment, around 23 ºC. The behavior of the sensor was also tested at different temperature values around that, using three pH levels (2, 7.4 and 10). For this purpose, a climatic chamber was used performing a temperature sweep from 20 ºC to 35 ºC, in steps of 5 ºC. The measurement was recorded with a stabilization time of approximately 10 minutes between each one, ensuring that both the chamber and the pH solution get to the target temperature. Fig 11. depicts the evolution of peak intensity at the target wavelength for the different pH samples.

This work is licensed under a Creative Commons Attribution-NonCommercial-NoDerivatives 4.0 License. For more information, see https://creativecommons.org/licenses/by-nc-nd/4.0/

This article has been accepted for publication in IEEE Sensors Journal. This is the author's version which has not been fully edited and
content may change prior to final publication. Citation information: DOI 10.1109/JSEN.2024.3419257

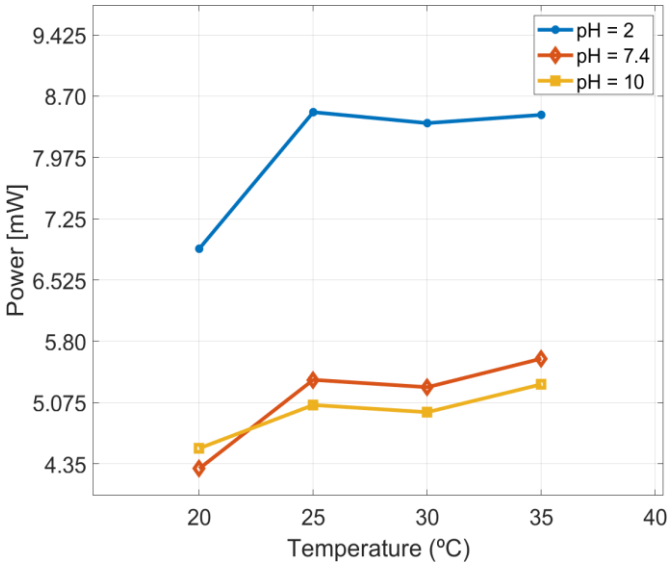

Fig. 11. Temperature variation influence in TCFF-based sensor.

The most significative changes are observed for temperatures below 25 ºC for all the samples, where the peak intensity changes abruptly. This is possible to occur due to the interaction of the thermal stabilization mechanism inside the chamber and the reaction of polyaniline with the pH samples.

The TCFF type of pH sensor has demonstrated an optimal temperature operation range above 25 ºC and can be adjusted according to application requirements.

In the case of D-shape fiber-based sensor, the temperature has practically no influence in the sensor response, as depicted in Fig. 12. A high stability is achieved in the full operation range.

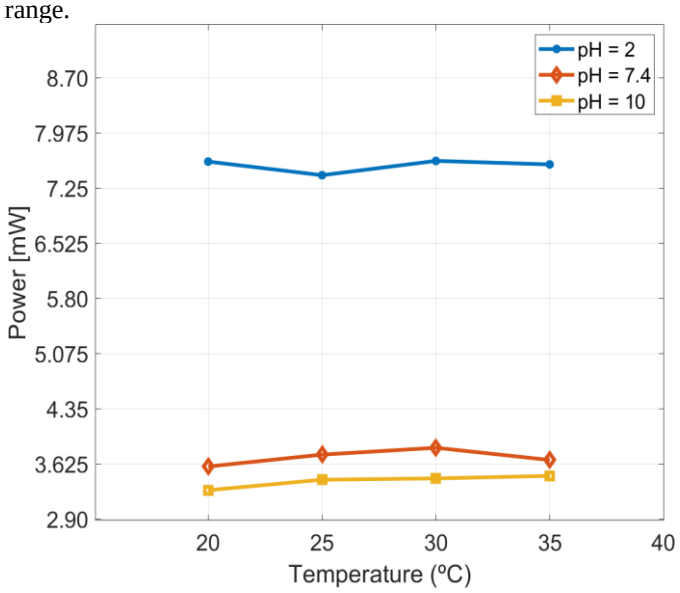

Fig. 12. Temperature variation influence in the D-shape fiber-based sensor.

IV. Conclusion

In this work, two optical fiber pH sensors using a TCFF and a D-shape fiber, both coated with polyaniline polymer were presented. This layer was produced *in situ* by coating the fiber surface via synthetic oxidative polymerization. The sensors achieved a variable sensitivity response, where the optimal operation zone, matching a linear trend, was between pH 4.2 and 8.1. In this range, the sensitivity measured was 1.06 mW/pH in terms of peak intensity for the trenched only bridge fiber.

The results were compared to the side-polished D-shaped fiber sensor. In this case, the linear sensitivity range was from 2.75 to 6.8, where the maximum variation achieved was 0.95 mW/pH.

The sensors were analyzed in multiple usages. The test was repeated in different days to check the response regarding the quality of PAni coating after polymerization time. The trenched only-bridge fiber showed the best response in terms of normalized transmittance, that increases around 10 % after the third test. However, the D-shape fiber achieved a significative change in pH levels above 7.1.

In terms of environmental cross-sensitivity, both sensors recorded did not show significant spectral response under temperature changes. In case of THCF-based sensor, a slight variation in peak power intensity was recorded for temperatures under 25 ºC, due to possible stabilization time mismatches.

The proposed sensor configurations can be further improved by combining both sensors and cover a higher range of pH measurements. The D-shape fiber for the low-pH zone and the TCFF for the high-pH zone, making a full pH 2.75 to 8.1 range. Moreover, in terms of cost-effectiveness of the system, the measurements can be performed using power meters to check the signal intensity losses as the pH increases.

Acknowledgment

The authors acknowledge CICECO-Aveiro Institute of Materials for the projects LA/P/0006/2020, UIDB/50011/2020 & UIDP/50011/2020, i3N projects UIDB/50025/2020, UIDP/50025/2020 and LA/P/0037/2020 and the project “DigiAqua” (PTDC/EEI-EEE/0415/2021), financed by national funds through the Portuguese Science and Technology Foundation/MCTES (FCT I.P., Portugal). The research was co-funded by the financial support of the European Union under the REFRESH – Research Excellence For Region Sustainability and High-tech Industries project number CZ.10.03.01/00/22_003/0000048 via the Operational Programme Just Transition. This work was also supported by the Ministry of Education, Youth, and Sports of the Czech Republic conducted by the VSB-Technical University of Ostrava, under grants no. SP2024/081 and SP2024/059.

References

[1] J. Werner, M. Belz, K.-F. Klein, T. Sun, and K. T. V. Grattan, “Fiber optic sensor designs and luminescence-based methods for the detection of oxygen and pH measurement,” *Measurement*, vol. 178, p. 109323, Jun. 2021, doi: 10.1016/j.measurement.2021.109323.

[2] P. Gou *et al.*, “Carbon Nanotube Chemiresistor for Wireless pH Sensing,” *Scientific reports*, vol. 4, p. 4468, Mar. 2014, doi: 10.1038/srep04468.

[3] V. Perumal, *pH Measurement using In House Fabricated Interdigitated Capacitive Transducer.* 2013.

[4] L. Manjakkal, S. Dervin, and R. Dahiya, “Flexible potentiometric pH sensors for wearable systems,” *RSC Advances*, vol. 10, no. 15, pp. 8594–8617, 2020, doi: 10.1039/D0RA00016G.

This work is licensed under a Creative Commons Attribution-NonCommercial-NoDerivatives 4.0 License. For more information, see https://creativecommons.org/licenses/by-nc-nd/4.0/

This article has been accepted for publication in IEEE Sensors Journal. This is the author's version which has not been fully edited and content may change prior to final publication. Citation information: DOI 10.1109/JSEN.2024.3419257

[5] P. Kraikaew, S. Jeanneret, Y. Soda, T. Cherubini, and E. Bakker, "Ultra-Sensitive Seawater pH Measurement by Capacitive Readout of Potentiometric Sensors," *ACS Sensors*, vol. XXXX, Feb. 2020, doi: 10.1021/acssensors.0c00031.

[6] M. S. Arefin, M. Coskun, T. Alan, A. Neild, J.-M. Redoute, and M. Yuce, *A MEMS Capacitive pH Sensor for High Acidic and Basic Solutions*, vol. 2014. 2014. doi: 10.1109/ICSENS.2014.6985373.

[7] Y.-Z. Juang, C.-F. Lin, H.-H. Tsai, H.-H. Liao, and R.-L. Wang, "CMOS Biomedical Sensor with In Situ Gold Reference Electrode for Urine Detection Application," *Procedia Engineering*, vol. 47, pp. 1005–1008, Dec. 2012, doi: 10.1016/j.proeng.2012.09.317.

[8] S. Singh and B. Gupta, "Fabrication and characterization of a highly sensitive surface plasmon resonance based fiber optic pH sensor utilizing high index layer and smart hydrogel," *Sensors and Actuators B: Chemical*, vol. 173, pp. 268–273, Oct. 2012, doi: 10.1016/j.snb.2012.06.089.

[9] S. Mishra and B. Gupta, "Surface plasmon resonance based fiber optic pH sensor utilizing Ag/ITO/Al/hydrogel layers," *The Analyst*, vol. 138, Mar. 2013, doi: 10.1039/c3an00097d.

[10] T. Nguyen, T. Venugopalan, T. Sun, and K. Grattan, "Intrinsic Fibre Optic pH Sensor for Measurement of pH Values in the Range of 0.5 – 6.0," *IEEE Sensors Journal*, vol. 16, pp. 1–1, Jan. 2015, doi: 10.1109/JSEN.2015.2490583.

[11] P. Zubiate, C. Zamarreño, I. Del Villar, I. Matias, and F. Arregui, *D-shape optical fiber pH sensor based on Lossy Mode Resonances (LMRs)*. 2015, p. 4. doi: 10.1109/ICSENS.2015.7370421.

[12] J. Corres, I. Matias, I. Del Villar, and F. Arregui, "Design of pH Sensors in Long-Period Fiber Gratings Using Polymeric Nanocoatings," *Sensors Journal, IEEE*, vol. 7, pp. 455–463, Apr. 2007, doi: 10.1109/JSEN.2007.891933.

[13] Y. Zheng *et al.*, "Miniature pH Optical Fiber Sensor Based on Fabry-Perot Interferometer," *IEEE Journal of Selected Topics in Quantum Electronics*, vol. 22, pp. 1–1, Jan. 2015, doi: 10.1109/JSTQE.2015.2497438.

[14] X. Cheng, J. Bonefacino, B. O. Guan, and H. Y. Tam, "All-polymer fiber-optic pH sensor," *Opt. Express*, vol. 26, no. 11, p. 14610, May 2018, doi: 10.1364/OE.26.014610.

[15] A. Lopez Aldaba, Á. González-Vila, M. Debliquy, M. Lopez-Amo, C. Caucheteur, and D. Lahem, "Polyaniline-coated tilted fiber Bragg gratings for pH sensing," *Sensors and Actuators B: Chemical*, vol. 254, pp. 1087–1093, Jan. 2018, doi: 10.1016/j.snb.2017.07.167.

[16] G. Lopes *et al.*, "Innovative optical pH sensors for the aquaculture sector: Comprehensive characterization of a cost-effective solution," *Optics & Laser Technology*, vol. 171, p. 110355, Apr. 2024, doi: 10.1016/j.optlastec.2023.110355.

[17] Y. Han *et al.*, "Side-polished fiber as a sensor for the determination of nematic liquid crystal orientation," *Sensors and Actuators B Chemical*, vol. 196, pp. 663–669, Jun. 2014, doi: 10.1016/j.snb.2014.02.076.

[18] Y. Chen, "A review of polyaniline based materials as anodes for lithiumion batteries," *IOP Conf. Ser.: Mater. Sci. Eng.*, vol. 677, no. 2, p. 022115, Dec. 2019, doi: 10.1088/1757-899X/677/2/022115.

[19] M. Beygisangchin, S. Abdul Rashid, S. Shafie, A. R. Sadrolhosseini, and H. N. Lim, "Preparations, Properties, and Applications of Polyaniline and Polyaniline Thin Films—A Review," *Polymers*, vol. 13, no. 12, Art. no. 12, Jan. 2021, doi: 10.3390/polym13122003.

[20] K. M. C. Tjørve and E. Tjørve, "The use of Gompertz models in growth analyses, and new Gompertz-model approach: An addition to the Unified-Richards family," *PLoS ONE*, vol. 12, no. 6, p. e0178691, Jun. 2017, doi: 10.1371/journal.pone.0178691.

[21] T. Khanikar and V. K. Singh, "PANI-PVA composite film coated optical fiber probe as a stable and highly sensitive pH sensor," *Optical Materials*, vol. 88, pp. 244–251, Feb. 2019, doi: 10.1016/j.optmat.2018.11.044.

This work is licensed under a Creative Commons Attribution-NonCommercial-NoDerivatives 4.0 License. For more information, see https://creativecommons.org/licenses/by-nc-nd/4.0/